NASA TECHNICAL NOTE

NASA TN D-3625

NASA TN D-3625




# PEGASUS THERMAL DESIGN


*by Tommy C. Bannister and Robert J. Eby*

*George C. Marshall Space Flight Center*
*Huntsville, Ala.*

NATIONAL AERONAUTICS AND SPACE ADMINISTRATION • WASHINGTON, D. C. • NOVEMBER 1966

# PEGASUS THERMAL DESIGN

By Tommy C. Bannister and Robert J. Eby

George C. Marshall Space Flight Center
Huntsville, Ala.

NATIONAL AERONAUTICS AND SPACE ADMINISTRATION

For sale by the Clearinghouse for Federal Scientific and Technical Information
Springfield, Virginia 22151 – Price $2.00

TABLE OF CONTENTS

LIST OF ILLUSTRATIONS

## LIST OF ILLUSTRATIONS (Concluded)



## LIST OF TABLES

## DEFINITION OF SYMBOLS

| Symbol | Definition |
|---|---|
| $q$ | Heat flux |
| $T$ | Absolute temperature |
| $T_s$ | Radiation sink temperature |
| $\xi$ | Radiation interchange factor |
| $\sigma$ | Stefan-Boltzmann constant |
| $A$ | Area |
| $F_e$ | Emissivity factor |
| $F_a$ | Configuration factor |
| $Q_C$ | Component heat generation |
| $k$ | Thermal conductivity |
| $K$ | Total thermal conductance |

# PEGASUS THERMAL DESIGN

## SUMMARY

Many of the components of the Pegasus spacecraft will function properly only so long as their temperatures are maintained within certain tolerances. The thermal requirements, thermal design, and orbital temperature results are presented.

When the temperature specifications were received, two areas were recognized to be critical: (1) the electronics and (2) the micrometeoroid detector panels. This report deals primarily with these aspects.

Analysis, design, testing, and flight data correlation are presented for the thermal control of Pegasus electronics. The temperature control was achieved by the use of an active louver system similar to that used on the Mariner spacecraft. The thermal design consists of a superinsulation envelope which completely surrounds the electronic components, with the exception of the one small opening or window over which the louvers are attached. The louvers control the heat flow from the electronic boxes, as a function of their temperature, to maintain temperatures between 280°K and 301°K throughout the one-year mission. The radiation heat sink consists of the Service Module Adaptor (SMA) and Saturn S-IV stage of the Saturn I booster. The exterior surfaces of the SMA and S-IV are coated with S-13 (zinc oxide pigmented methyl silicone elastomer). Adaption of the louver system to a randomly tumbling vehicle is discussed. Thermal control cannot be attitude dependent. Safe component temperature levels must be maintained for any spacecraft orientation.

A seven-node mathematical thermal model of the electronics is described by seven simultaneous equations. Separate multinode analyses were conducted to determine structural and skin sink temperatures. Also, a 45-node analysis was made to verify the working model. This model was not used exclusively because of long computer time requirements.

Thermal vacuum orbital simulation tests are described. These tests were conducted using live electronics mounted in a section of the Pegasus structure modified to fit the chamber. Orbital sink temperatures corresponding to incident radiant fluxes were applied to the structure and electronics through the use of 34 zoned heating blankets.

The 23 temperature sensors mounted on each Pegasus spacecraft have been monitored since launch. Correlation with analytical and experimental results has been excellent, and a portion of these data is presented. It is noted here that the specified orbital eccentricity was changed after the thermal concepts for temperature control of the electronics canister was formed. This had the effect of lowering the maximum expected heat sink temperatures. (The maximum value of the percentage time per orbit in sunlight was reduced.) Further preflight analysis showed that the louver concept was still acceptable, the only effect being that the louvers would probably never be opened a full 90°; however, the louvers were still necessary. As it turned out, the unexpected 40° K increase in the heat sink temperatures on each of the three Pegasus' served only to shift the angular operating range of the louvers. Hence, the temperature of the electronics canister was virtually unaffected. However, it can be postulated that the electronic canister temperatures would have exceeded their upper design limit if the original orbit had been used. This point will not be elaborated on any further in this report as it is only intended to present the thermal design effort of Pegasus and to show flight results only on a quick-look basis. A detailed postflight thermal analysis is in progress at the Research Projects Laboratory of Marshall Space Flight Center where reports are forthcoming. The preflight analysis given in this report is based upon the final specifications.

A description of the thermal design of the Pegasus micrometeoroid detector panels is presented. Analysis is based on a four-node, one-dimensional heat balance analysis where the only controllable parameter for temperature control is the radiometric properties of the panels exterior surface. Vacuum testing and flight data are discussed.

# INTRODUCTION

The Pegasus satellite (Fig. 1), formerly called the Micrometeoroid Measurement Capsule, was developed by the Fairchild-Hiller Corporation* under the supervision of the Marshall Space Flight Center (MSFC), Huntsville, Alabama. Pegasus-A was injected into orbit February 16, 1965, by SA-9; Pegasus-B was orbited May 25, 1965, by SA-8; Pegasus-C was orbited by SA-10 July 30, 1965. The primary mission of these spacecraft is the micrometeoroid measurement experiment designed to obtain statistical data on micrometeoroids. The satellite is required to have a large micrometeoroid detection area, a long lifetime (about 12 to 18 months), and a slowly changing random orientation in space. The planned orbital characteristics of Pegasus A and B were a perigee of 486.9 km, an apogee of 747.7 km, and a period of 97.14 minutes. The Pegasus-C orbit was designed to be slightly more circular. The actual elements of Pegasus-A were a 496.4-km perigee, a 743.5-km apogee, and a 97.10-minute period. Initially, Pegasus-A was spinning about its longitudinal axis (X-axis). Since the X-axis is not the principle moment of inertia, the satellite began to precess, with the angle of precession gradually increasing until the only mode of spin became the mode about the principle moment of inertia (the Y-axis, which is normal to the detector surface). This transition was completed within approximately eight days after the launch of Pegasus-A.

Pegasus B and C, however, are displaying unexpected spin motion in orbit. Pegasus B and C, like Pegasus-A, were given initial spin about the longitudinal axis of the S-IV stage and subsequently began to precess. When the precession angle reached about 20 degrees, it ceased to change appreciably (Pegasus-A opened up to 90 degrees within about eight days). This phenomenon is being investigated by the Orbital Mechanics Group at MSFC.

In addition to the meteoroid detection system, support functions of the mission include subsystems for providing power; processing data; measuring temperatures, voltages, currents, and ionizing radiation; determining attitude; and a provision for telemetered communications. These components are grouped in and supported by the electronics canister located in the thermally controlled area at the lower end of the center section. Each functional unit is separately packaged

* Formerly Fairchild-Stratos Corp.

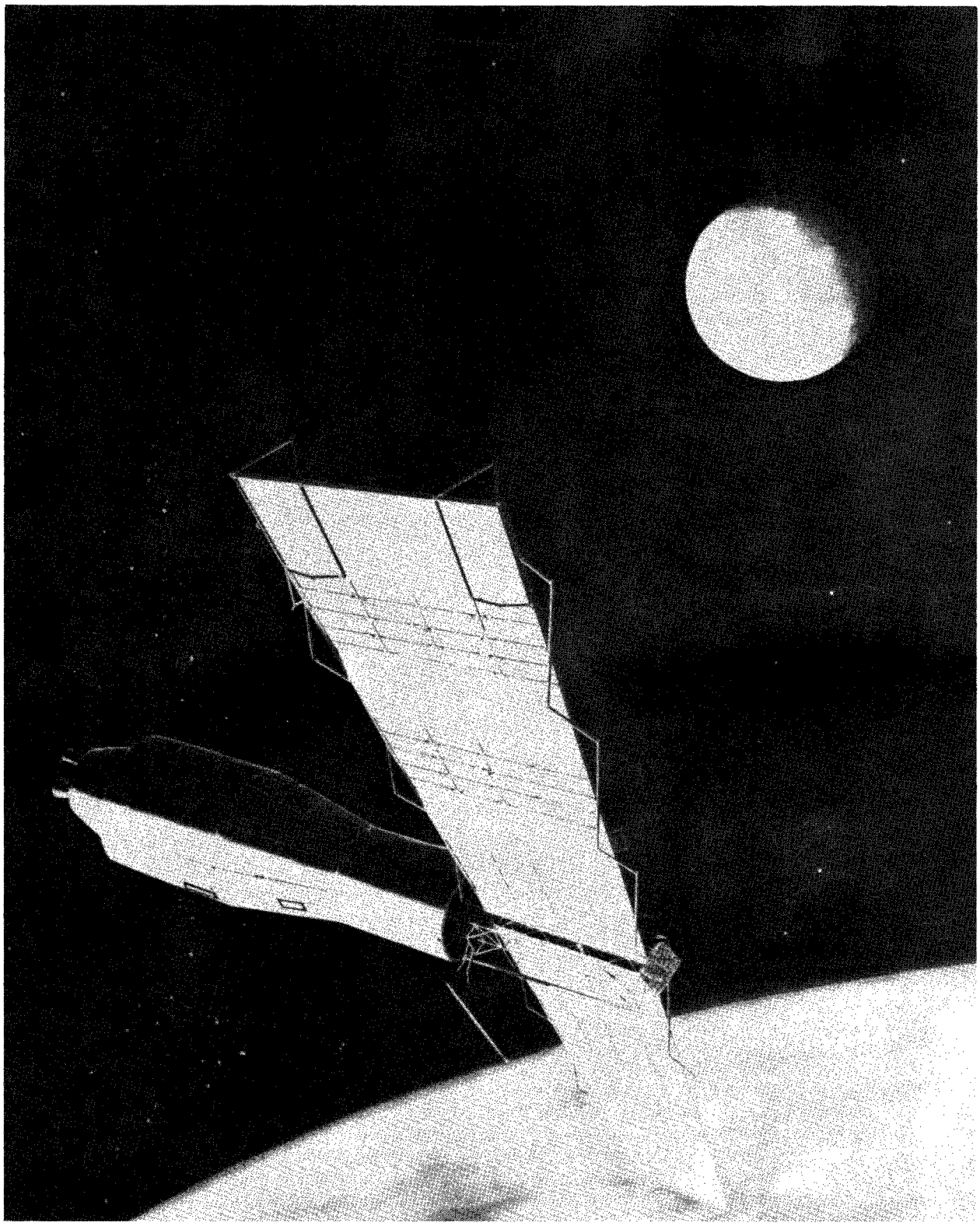

FIGURE 1. PEGASUS SATELLITE

in an RFI-shielded* box and mounted on a double "Y" shaped frame. The structure frame is covered on five sides by superinsulation blankets. On the bottom side, it is covered by two sets of louvers covering an area of 0.32 square meters. Each louver is separately controlled by a bimetallic spring; this provides a reliable thermal control on a zoned basis.

The first consideration in the thermal design was to obtain the thermal specifications of the various components of the spacecraft, and to become familiar with the thermal requirements of the mission and hardware. Compatible thermal design concepts and criteria could thereby be formulated which would not interfere unnecessarily with other design areas.

Because of functional and material thermal limitations, the micrometeoroid detector panels and the electronics were the critical areas for thermal design. The problem associated with the detector panels was the possibility of severe thermal variations that conceivably could cause panel delamination. A detailed study of this problem revealed that the only readily controllable parameters were the optical properties of the panel's exterior surfaces. The orbital temperatures were defined for all sets of possible optical properties. A search for the coating with suitable optical properties resulted in the selection of the chemical conversion coating, Alodine. This coating was subjected to ultra-violet radiation in the laboratory to verify the space stability of its properties. Also, a detector panel was studied in a thermal space chamber at hard vacuum.

The thermal problem associated with the electronics is ensuring that the temperatures do not exceed the prescribed "upper" and "lower" limits. The temperatures of most electronic components are a strong function of internal heating rates, thermal linkage to the supporting structures, structure temperature, and radiation heat transfer to other parts of the spacecraft and to space. Several of these have been controlled, to a degree, by design. Where possible, the electronic components were placed in a thermally insulated canister (Fig. 2) with a "sized window" to radiate the internally generated heat to a cold sink. This window faces the vehicle to eliminate direct solar radiation into the canister. With random orientation, such a variable input as the direct solar radiation would greatly increase the design requirements.

Throughout this report the terms "SMA" and "sink" are used interchangeably when speaking of the canister radiation heat sink. The SMA is an adaptor to the Service Module. The window sees the internal areas of the SMA, Instrument Unit (IU), and S-IV stage bulkhead (Fig. 3).

*RFI - radio frequency interference

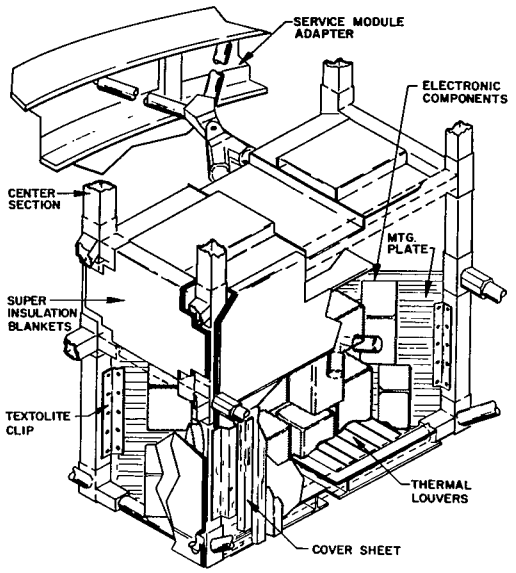


FIGURE 2. ELECTRONIC CANISTER

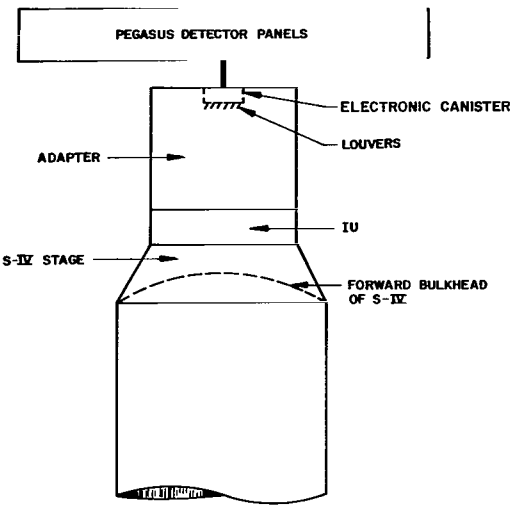


FIGURE 3. OPEN END OF THE VEHICLE AS A TEMPERATURE SINK

Since most of the factors affecting the canister thermal design are variable, and the thermal time constant is obviously large, it is useful to consider a thermodynamic "hot" and the thermodynamic "cold" case. If the varying factors are not too severe, the window could be sized to keep both the hot and cold cases within specified limits. Hence, with moderate parameter variations, the steady-state hot and cold extreme temperatures can each be kept within the design range. In the case of Pegasus, this was determined an inadequate method of control. After several alternatives were evaluated, an active louver system (Fig. 4) was employed which prohibits radiant heat flow through the window in the cold case (blades closed), without much hindrance to the heat flow in the hot case (blades open).

## HARDWARE DESCRIPTION

The electronic canister is positioned in the lower portion of the center section, as indicated in Figure 5. The double Y shaped canister is bolted to the four vertical center section members by textolite clips. The clips were designed to provide high thermal resistance to heat flow by conduction from the warm components to the relatively cold structure. Radiative heat transfer is restricted by the use of superinsulation blankets on each side except the bottom. The blankets consist of ten sheets of aluminized mylar one-fourth mil thick sandwiched between an inner mylar support card and outer aluminum face sheet. The face sheets are coated with S-13 thermal coating. A cutaway view of the canister is shown in Figure 2.

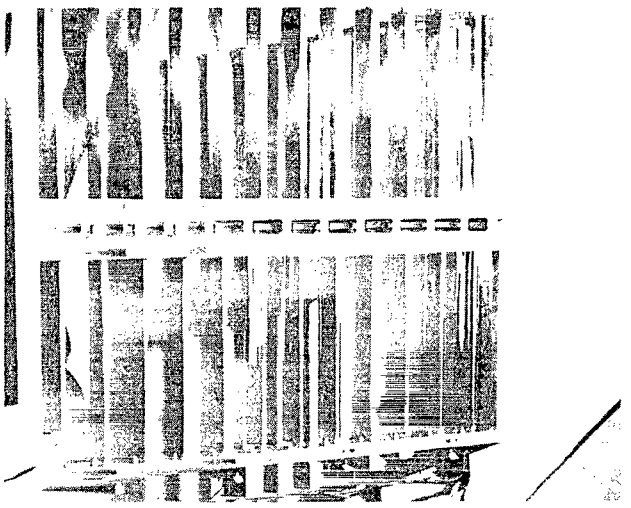

FIGURE 4. THERMAL CONTROL LOUVERS

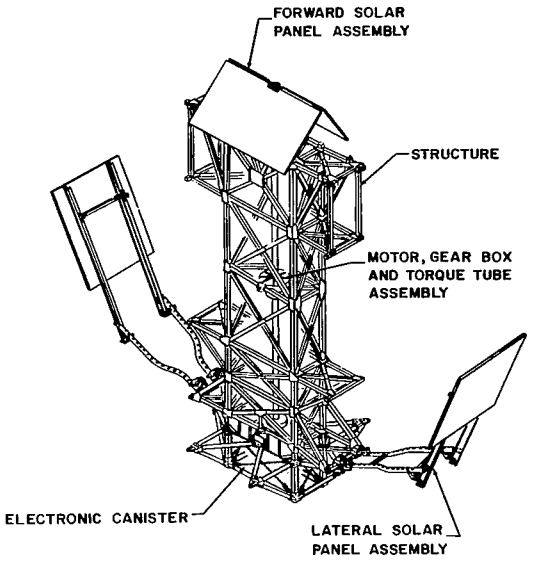


FIGURE 5. PEGASUS CENTER SECTION

The micrometeoroid detector panel consists of a hard polyurethane foam core with a layer of soft polyurethane foam bonded to each side of the hard case. The detector capacitors are then bonded to the soft foam. This design minimizes the effect of thermal stress. A panel is 0.5 m × 1.0 m × 2.4 cm. The hard core is about 1.25 cm thick, and each soft foam layer is about .6 cm. The capacitors consist of a thick aluminum panel with a very thin dialectric layer and a very thin copper layer deposited on the aluminum such that, thermally, the capacitor can be considered a panel of aluminum. There are three thicknesses of aluminum capacitors: 16 mil, 8 mil, and 1.5 mil.

## THERMAL REQUIREMENTS OF PEGASUS IN ORBIT

A list of thermal specifications for the components of Pegasus was prepared by the contractor; the thermal requirements follow.

a. Electrical components

1. Inside the canister

| | |
|---|---|
| Batteries | 272°K to 322°K |
| Others | 262°K to 332°K |

2. Outside the canister

| | |
|---|---|
| Zener diodes | 218°K to 358°K |
| Solar cells | 194°K to 339°K |

b. Other components

| | |
|---|---|
| 1. Micrometeoroid detector panels | 167°K to 394°K and $\dot{T}$ less than 100°K/min. |
| 2. Infrared sensors | 218°K to 358°K |
| 3. Radiation detector | 222°K to 388°K |

# THERMAL DESIGN

## Analysis

Thermal design of the electronic canister. -The analysis of the electronic canister consisted of a primary analysis of representative average heat balance equations, and detailed studies for validation accomplished through a complex computer program.

The canister (Fig. 2) was designed to be thermally isolated for the following reasons: (1) to prevent the components from being thermally linked to heat sources of temperatures difficult to determine, such as the Pegasus center structure; (2) to insure that the components will not be affected by varying radiant sources of heat, such as direct solar radiation; and (3) by minimizing extraneous heat transfer, the "controllable" heat transfer is maximized. Therefore, the difference in controllable heat transfer between the hot and cold cases is minimized. This is most important because it is basically this difference that determines the amount of active thermal control required. (With zero difference, the area of the open face could be simply sized to give the proper temperature, or with a very large difference, louvers would not accomplish thermal control.)

The techniques employed to obtain this thermal isolation follow. The canister side walls were equipped with ten layers of super-insulation,* consisting of highly reflective sheets of aluminized mylar, which greatly restrict

*Mr. Jack Light at National Research Corp. was employed as advisor in the use of superinsulation.

radiant heat transfer through the side walls. The internal mounting bracket for the components was formed as a double Y and attached to the supporting structure with special fiberglass chips to restrict heat conduction to the center structure. The connecting cables and possible radiant heat-leakage areas were covered with a low-emittance aluminized mylar tape, which minimized the radiant linkage between the canister components and certain cold structures.

During an orbital cold case, the louvers will be closed and reflect incident energy to maintain minimum component temperature levels. In the hot case, the blades will be open, permitting the expulsion of radiant heat to the external cold sink (SMA, IV, and S-IV stage).

The coating selection minimized the temperature drop between the hot heat-dissipating components and the cold non-dissipators. Because of a severe weight penalty, it was undesirable to employ a thermally conductive mounting plate which would distribute heat by conduction.

Heat balance analysis. -In systems with large thermal time constants, the average heat balance analysis generally can be used without difficulty. Care must be taken to ensure that erroneous results are not obtained in an over-simplified model. The analysis employed in the thermal design of the Pegasus electronics canister was carefully worked out, and later verified by more detailed computer studies and thermal vacuum tests.

Two of the dominant heat inputs vary primarily because of eclipse of the sun by the earth. It is useful, therefore, to define $T_x$ as the percentage of time-in-sunlight per orbit. For the Pegasus orbit, the range of $T_x$ is 63 percent to 78 percent, calculated by W. C. Snoddy, MSFC, and calculations by Fairchild-Hiller Corporation. The internal heat generation of the electronics depends upon $T_x$ primarily because the solar cell output depends on the amount of incident sunlight. Also, the solar radiation absorbed by the external satellite surfaces depends strongly on $T_x$.

The prelaunch internal heat generation (the second dominant factor) was determined to be 45W to 63W, when averaged over one orbital period.

Now the $T_x$, together with the following attitude consideration, is used to determine the sink temperature as a function of the radiometric or optical properties of the SMA, IU, and S-IV stage external surfaces.

Perhaps the most important consideration in the thermal design of the Pegasus canister is solar attitude. Obviously, if the long cylindrical SMA, IU, and S-IV stage become oriented with the rear of the S-IV stage toward the sun,

the sink temperatures ($T_{s1}$) sill become very low. If this never occurs during any appreciably length of time, the range of $T_{s1}$ is substantially reduced. A special "thermal factor" was calculated by the Physics and Astrophysics Branch, R-RP-P, which performed the prelaunch attitude analysis of the Pegasus. This factor represents the average projected area of the sink over various time periods and was calculated for the many possible orbital situations. Therefore,

$$\underline{\gamma} = \frac{1}{t} \int_0^t \sin\theta \, dt$$

$$\lim_{t \to \infty} \gamma = 2/\pi$$

where

$\theta$ = sun angle of the longitudinal axis of the S-IV

t = time

$\underline{\gamma}$ = thermal factor.

In all attitude cases considered, $\Upsilon$ was never less than 0.6 for t within the thermal time constant, indicating that the tumble period was always less than the thermal time constant (15 hours). This is of tremendous consequence for Pegasus because the range of $T_{s1}$ would otherwise be about three times the present value, and the present thermal design would be inadequate. Analytically, this means that the average projected area to the sun (essential to the evaluation of $T_{s1}$) will be identical to that calculated for a rapidly tumbling cylinder.

Significant mathematical simplification in the heat balance equations is achieved by making use of the large thermal time constants associated with the structure, superinsulated electronics canister, and adaptor. The time constant of the electronics varies from about 30 hours in the cold case (louvers closed) to over 15 hours in the hot case* (louvers open). This variation, together with the isothermal packaging concept, means that component dissipation can be

*A second hot case with the sun looking into the open adaptor (along +X axis) was considered and found to be slightly less severe. In this case, the shadowing effect of the forward solar panels is significant in reducing the total incident flux.

averaged over relatively long time periods, and that peak or spike dissipation loads need not be considered in the analysis. It is, therefore, possible to use orbital average heating fluxes and the corresponding sink temperatures. It follows that the canister temperature is virtually invarient during a given orbit; there is no significant temperature decrease during shadow periods.

In determining the orbital heat sink temperatures, it was possible to neglect the dissipation of the electronics. Relative to the impinging, solar, albedo, and earth fluxes, the component dissipation flux is small and has negligible effect on the heat balance computations related to the structure, SMA, Instrument Unit, and S-IV stage. For this reason, the orbital temperatures of these items was computed separately and used as inputs for the canister mathematical model. Consequently, the canister analysis was greatly simplified, and parametric studies involving conductivities, emissivities, louver area, and thermal dissipation could be handled readily during the early design and development stages of the program.

The notation used for the mathematical model corresponds to Figure 2. The symbols are defined below:

$T_{s1}$ = Adaptor radiative sink temperature

$T_{s2}$ = Center section structure conduction sink

$T_{s3}$ = Adaptor support structure conduction sink

Node 1 = Outside surface insulation blanket (top section)

Node 2 = Inside surface insulation blanket (top section)

Node 3 = Electronic components

Node 4 = Inside surface insulation blankets (sides)

Node 5 = Outside surface insulation blankets (sides)

Node 6 = Louver frame

Node 7 = Center section side of insulating clip.

A schematic of the thermal circuit is shown in Figure 6. The steady-state heat balance equation for each node are:

1. $F_{e1\text{-}s1}F_{a1\text{-}s1}A_{1\sigma}(T_1^4 - T_{s1}^4) = F_{e2\text{-}1}F_{a2\text{-}1}A_{2\sigma}(T_2^4 - T_1^4)$

2. $F_{e3\text{-}2}F_{a3\text{-}2}A_{3\sigma}(T_3^4 - T_2^4) = F_{e2\text{-}1}F_{a2\text{-}1}A_{2\sigma}(T_2^4 - T_1^4)$

3. $K_{3\text{-}7}(T_3 - T_7) + F_{e3\text{-}s1}F_{a3\text{-}s1}A_{3\sigma}(T_3^4 - T_{s1}^4) + F_{e3\text{-}6}F_{a3\text{-}6}A_{3\sigma}$

$(T_3^4 - T_6^4) + F_{e3\text{-}2}F_{a3\text{-}2}A_{3\sigma}(T_3^4 - T_2^4) + F_{e3\text{-}4}F_{a3\text{-}4}A_{3\sigma}(T_3^4 - T_4^4) = Q_c$

4. $F_{e3\text{-}4}F_{a3\text{-}4}A_{3\sigma}(T_3^4 - T_4^4) = F_{e4\text{-}5}F_{a4\text{-}5}A_{4\sigma}(T_4^4 - T_5^4)$

5. $F_{e4\text{-}5}F_{a4\text{-}5}A_{4\sigma}(T_4^4 - T_5^4) = F_{e5\text{-}s1}F_{a5\text{-}s1}A_{5\sigma}(T_5^4 - T_{s1}^4)$

6. $F_{e3\text{-}6}F_{a3\text{-}6}A_{3\sigma}(T_3^4 - T_6^4) = F_{e6\text{-}s1}F_{a6\text{-}s1}A_{6\sigma}(T_6^4 - T_{s1}^4)$

7. $K_{3\text{-}7}(T_3 - T_7) = K_{7\text{-}s2}(T_7 - T_{s2}) + K_{7\text{-}s3}(T_7 - T_{s3})$ .

Using boundary conditions determined for the hot and cold cases, the above equations were solved to find the component temperature (Node 3) as a function of the louvered area. From the results shown plotted in Figure 7, the optimum area was chosen as .32 square meters. Corresponding to this area, the component operating range is between 280°K and 301°K.

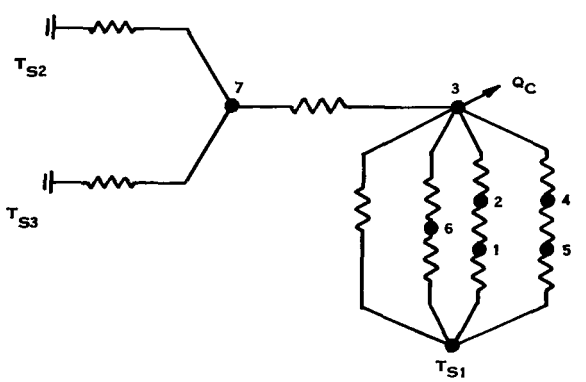


FIGURE 6. THERMAL CONTROL SCHEMATIC

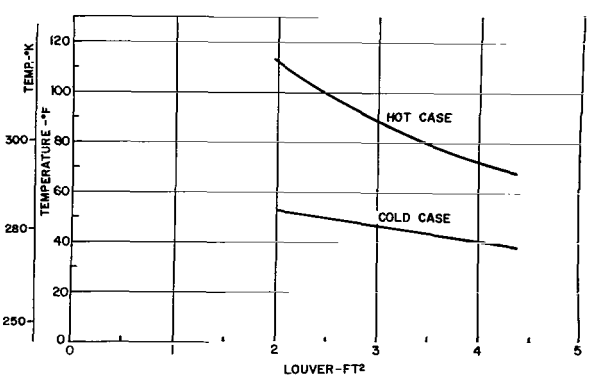


FIGURE 7. AVERAGE COMPONENT TEMPERATURE VERSUS LOUVER AREA

Effective hemispherical emissivity of the louvers was taken as 0.15 for the closed position and 0.65 for the open. The emissivity relationship as a function of the blade opening angle was assumed to vary as

$$F_e = 0.65 \cos (-0.851\theta + 76.6) \quad .$$

This relation agrees well with the predicted analytical results of Plamondon corresponding to a component (back surface) emissivity of 0.9 and a blade surface emissivity of 0.05 [1]. In the closed position, the effective emissivity is higher than that which was determined for the ideal system because of the existence of radiation gaps between the individual blades and the frame at the sides and ends, and because of conduction losses that exist at the frame mounting points.

Figure 8 shows how the average component temperature varies with the average orbital power dissipation of the components. The uppermost curve is for the hot case (blades fully open); the lower curve is based on the cold case (blades closed). Corresponding to a minimum dissipation of 45 watts in the cold case, the average temperature is 280°K. In the hot case, the maximum average dissipation is 62 watts, and the maximum component temperature is 300°K.

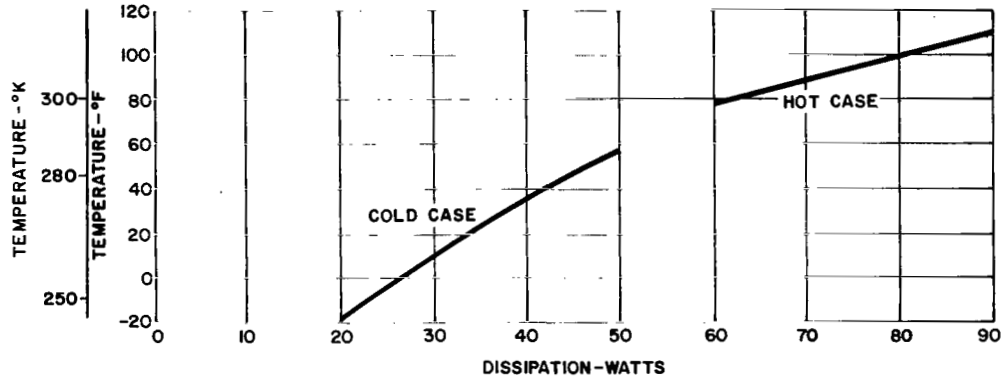


FIGURE 8. AVERAGE COMPONENT TEMPERATURE VERSUS DISSIPATION

Percentage sun-time variation over the year has been computer-based on various launch hours and the January 1 launch (Fig. 9). The day of year has little effect; however, the launch hour is significant in determining when maximum and minimum percentage sun-time occurs.

These computations show that the time periods spent in cold orbits with minimum percentage sunlight and in hot orbits with maximum percentage sunlight

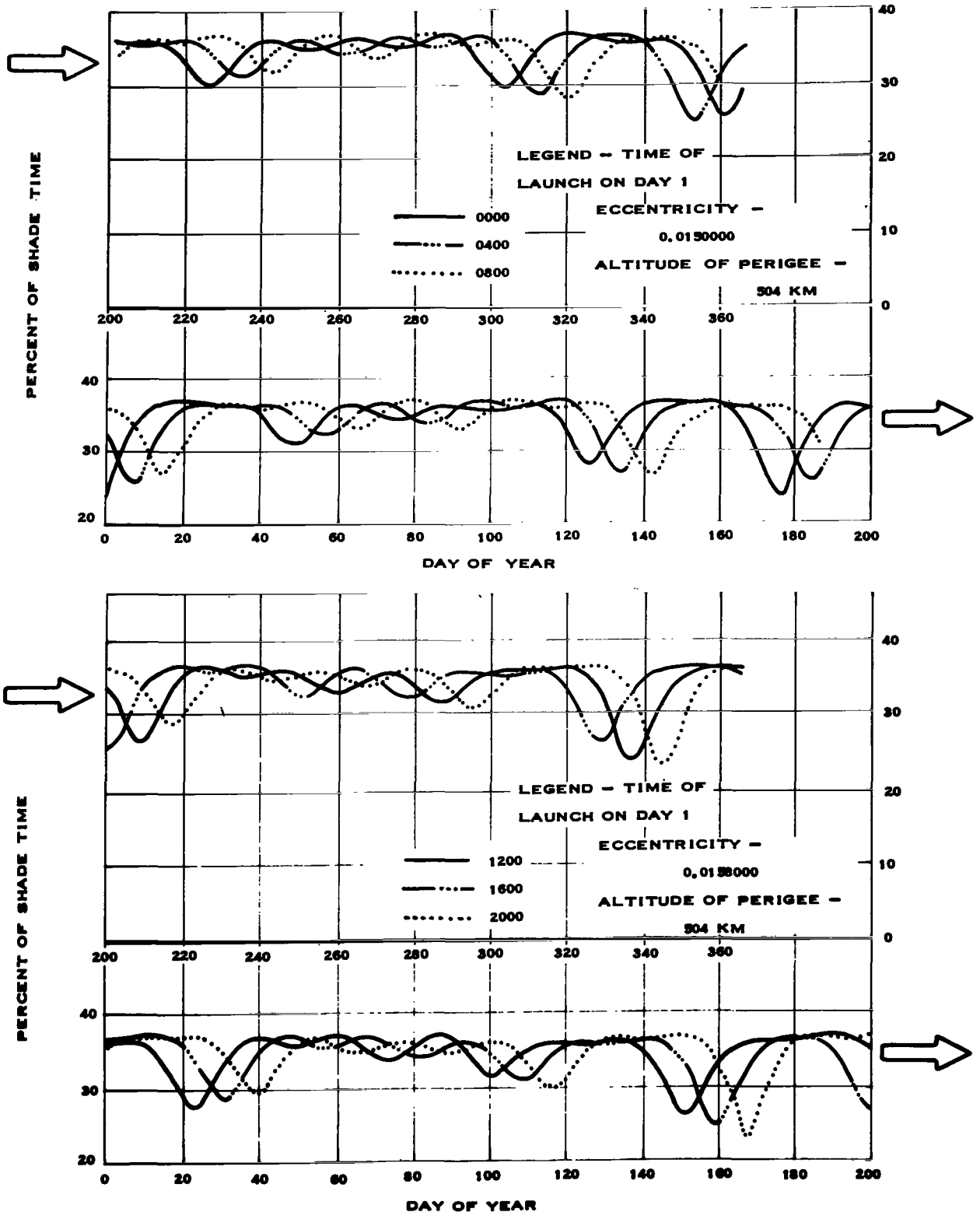


FIGURE 9. SHADE TIME VERSUS DAY OF YEAR

are large compared with the thermal time constant of the system. This means that no degree of conservatism is inherent in percentage sun-time variation allowance.

45-node analysis of the electronics canister. -This analysis evaluated the calorimetric heat-balance equations without resorting to the use of averaging; the thermodynamic model was broken down into 45 nodes with 45 simultaneous first-order differential equations. These equations are solved on the IBM 7090 Model II, utilizing the General Space Thermal Program developed at Marshall by W. C. Snoddy and Tommy C. Bannister. The sink temperature range obtained was 209° K to 240° K. Several runs were made using various values of the parameters directly affecting the canister temperatures. The results were very similar to those obtained by using the average heat-balance calculations.

Louver failure analysis. -Bimetallic actuators are used to position the louver blades. These actuators produce a torque functionally dependent on their temperature. Pegasus louver actuators are set to open the blades fully when their temperature reaches 286° K. The blades are fully closed at an actuator temperature of 263° K.

In orbit, the average actuator temperature will be proportional to the average component temperature. Since the allowable component temperature range is from 272° K to 322° K and the actuator range is from 263° K to 286° K, it follows that the actuators are designed to open and close the blade with a considerable temperature margin with reference to the allowable component temperature. This margin was split between the hot and cold case extremes so that the blades will be fully opened long before the hot case extreme is reached and fully closed before the cold extreme is reached. To visualize the operation, it is necessary to recall that the canister time constant is a matter of hours; the actuators react in minutes to a change in their environment. In this sense, the louvers act as a valve in an ON-OFF system.

From the preceding discussion, it is evident that intermediate louver blade positions are not critical and will not influence temperature control at the extremes. If alignment tolerances and bearing friction cause some blades to react more slowly and close or open later, the thermal performance will not be affected.

An analysis was conducted to determine the effect of louver blade failure on the average component temperature. Each spacecraft contains a total of 24 louver blade sets. In multiples of two, the blades were assumed to fail to maximize the temperature change, i.e., in the hot case, blades were assumed to fail while in a closed position; in the cold case, they were open. The results are

shown in Figure 10; the minimum allowable temperature of 272° K was maintained with three blades that failed in open position. In the hot case, 322° K was not exceeded when 14 blades failed in a closed position.

The average component temperature as a function of louver blade opening angle was investigated. The analysis was based upon an assumed case where all blades become locked at the same angle regardless of thermal conditions. The analysis applies only to this unlikely type of failure or malfunction, since for normal operation, the blades will be completely closed in the cold case and fully open in the hot. Thus, the lower curve in Figure 11 gives the component temperature during the cold environmental extreme for various blade angles from the completely closed position. Similarly, the upper curve applies only to the hot extreme and shows the effect of the louver's remaining partially closed. It must be noted that all blades are assumed to fail in the same angular position. Although this type of failure is practically an impossibility, the curves do provide an additional parameter for evaluating the sensitivity of the system.

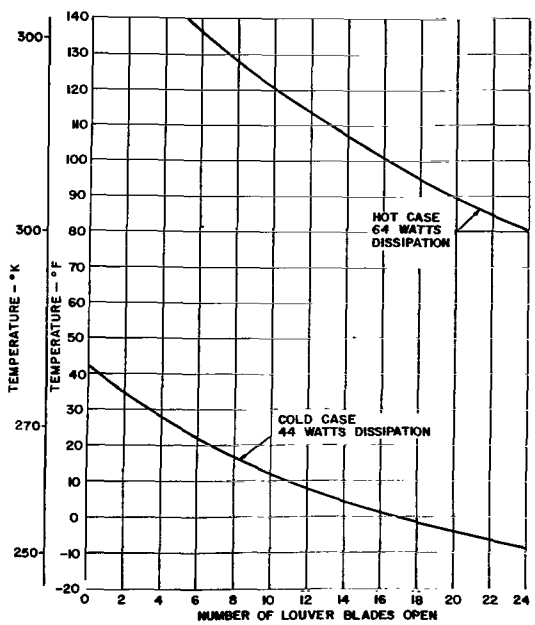


FIGURE 10. AVERAGE COMPONENT TEMPERATURE VERSUS NUMBER OF LOUVER BLADES OPEN

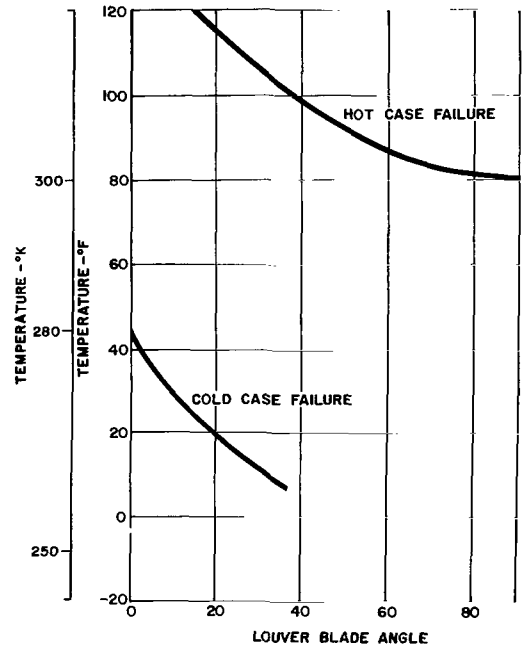


FIGURE 11. COMPONENT TEMPERATURE VERSUS LOUVER BLADE ANGLE HOT AND COLD

Thermal analysis of the micrometeoroid detector panels. -Unlike the electronics canister, the detector panels (Fig. 12) possess a very small thermal time constant (on the order of ten minutes). This causes rapid thermal fluctuations of the earth's shadow at various solar angles. Since hand calculations are impractical in an analysis where high rates of change must be considered, the

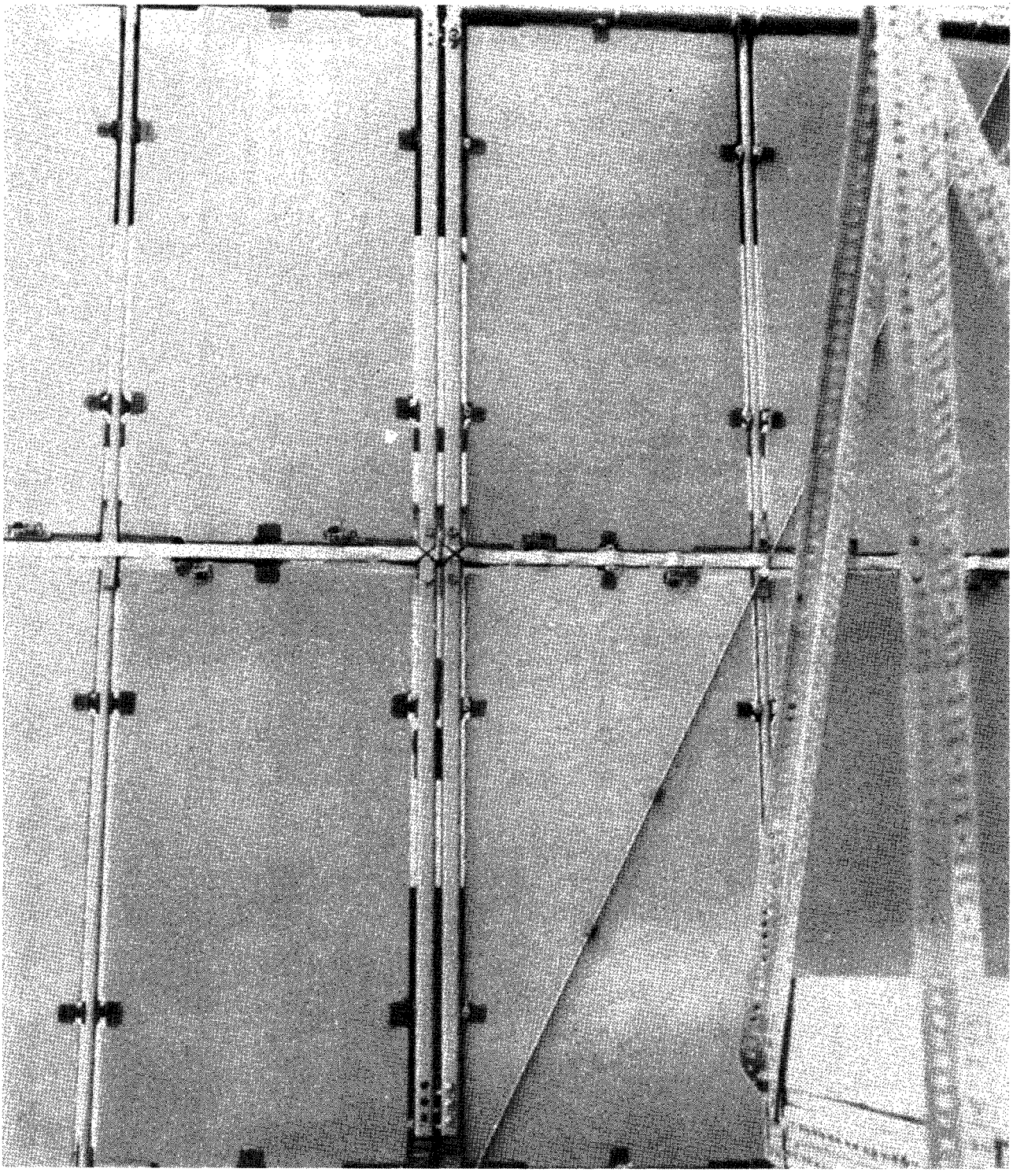

FIGURE 12. MICROMETEOROID DETECTOR PANELS

computer was used exclusively for defining the temperature excursions in orbit for the detector panels. The computer analysis is based on a four-node thermal model having the following characteristics:

a. The panel is an infinite slab of foam 2.54 cm thick (one-dimensional heat flow analysis)

b. Foam density - 480 Kg/$m^2$

c. Specific heat - 1350.0 joules/Kg° K

d. Foam thermal conductivity - 0.015 watts/m° K at 200° K
0.041 watts/m° K at 300° K
0.137 watts/m° K at 400° K

e. The slab is considered to have four equal layers of material. (The heat capacity of the aluminum target sheets is included in the outside layers.)

f. $\alpha_s$ and $\epsilon_T$ are floating parameters.

This model is adapted to the General Space Thermal Program (Article I and II, Appendix I) from which typical curves were obtained, as shown in Figure 13.

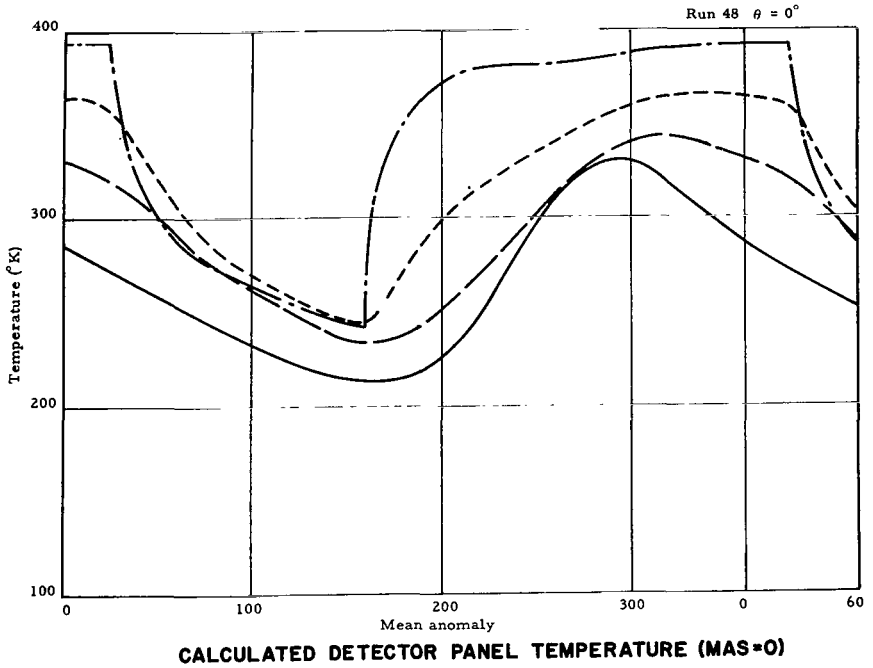


FIGURE 13. ORBITAL DETECTOR PANEL TEMPERATURE

Figure 13 represents the solar broadside which is the extreme hot case. Figures 14 and 15 show maximum and minimum possible detector panel temperatures versus $\alpha_s/\epsilon_T$.

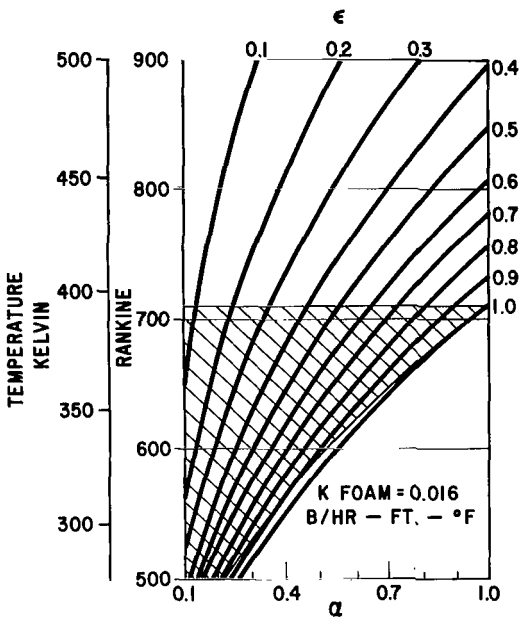


FIGURE 14. MAXIMUM DETECTOR PANEL TEMPERATURE VERSUS $\alpha_s/\epsilon_T$

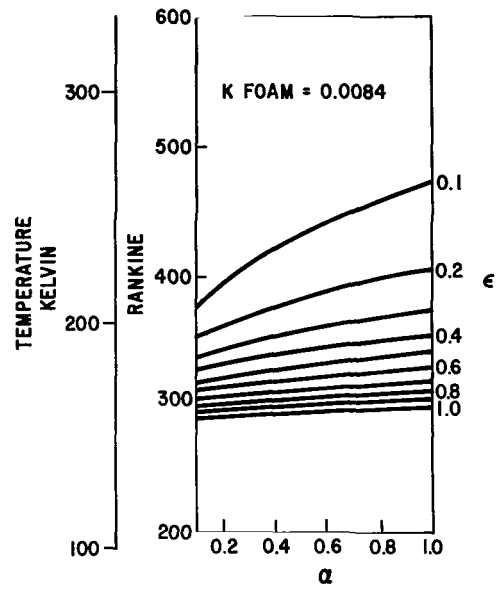


FIGURE 15. MINIMUM DETECTOR PANEL TEMPERATURE VERSUS $\alpha_s/\epsilon_T$

Examination of the results showed that a low $\alpha_s/\epsilon_T$ minimizes the maximum temperature, and a low $\epsilon_T$ maximizes the minimum temperature. The limiting values required to keep the temperatures within the design limits were $\alpha_s/\epsilon_T \leq 1$ and $\epsilon_T \leq .6$. The space stable chemical conversion coating, Alodine, was developed which exhibited properties consistent with these specifications, and which was relatively inexpensive (compared to other coatings such as vacuum deposition of SiO on approximately 200 $m^2$ of detector surface). Nominal values of $\alpha_s/\epsilon_T$ were .5/.6. A few panels had $\alpha_s/\epsilon_T$ from .4/.6 to .5/.5.

Other thermal analyses. -Design or allowable temperature limits for the electronic components located exterior to the canister were dictated by functional and/or material limitations. Thermal control for these items, which include the solar and IR sensors, zener diodes, spectrometer and solar panels, was provided on a passive basis. In most cases, multinode transient analyses were performed to determine the optical properties of a suitable thermal coating. Thus, by the selection of coatings and, in most cases, thermal isolation from the supporting structure, design temperature limits are maintained.

Predicted maximum and minimum temperatures are based on worst-case spacecraft attitude, together with degraded optical properties which could exist at the end of the mission. These temperatures are listed below:

| Item | Component Temperature Extremes (Minimum) | (Maximum) |
|---|---|---|
| IR sensors | 261°K | 352°K |
| Zener diodes | 218°K | 358°K |
| Spectrometer | | |
| sensor | 233°K | 311°K |
| electronics | 232°K | 325°K |
| Solar panels | 194°K | 339°K |

## Thermal Coating Selection

It was necessary to select a thermal control coating which would minimize the temperature of the heat sink to which the electronic components radiate heat. To see the first-order effect of this sink temperature, the following expression is considered.

$$q = \xi(\sigma T^4 - \sigma T_{s1}^4)$$

where

q = heat flux

T = average temperature of controlled body

$T_{s1}$ = radiation heat sink temperature

$\xi$ = radiation interchange factor

$\sigma$ = Stefan-Boltzmann constant.

It is apparent that as $T_{s1}$ is minimized so that $\sigma T_{s1}^4$ is small compared with $\sigma T^4$, the variation of $\sigma T_{s1}^4$, due to percentage sunlight variation and coatings absorptivity increase, will have small effect on the heat liberated. It follows then that T will be a major function of q and close temperature control may be maintained.

$T_{s1}$ may be minimized by the selection of a thermal coating with a low absorptivity ($\alpha_s$) and high emissivity ($\epsilon_T$). The problem was to find a coating with these optical properties which would remain stable under long-term solar (ultraviolet) exposure. For long-term missions, in the neighborhood of one year, degradation leading to an increase in $\alpha_s$ is considerable for almost all known flat reflectors (low $\alpha_s/\epsilon_T$ coatings).

After careful evaluation, S-13 (zinc oxide pigmented methyl silicone elastomer) was chosen as the thermal control coating for the heat sink. The nominal $\alpha_s$ is 0.22, and it can be expected to degrade to only 0.26 after 1800 equivalent sun-hours. The emittance is in excess of 0.85 for a 4- to 5- mil thick coating. S-13 was developed at the Illinois Institute of Technology (IIT) and tested extensively there and at both Fairchild-Hiller and MSFC for ultraviolet degradation behavior. The Pegasus is the first spacecraft to use S-13, which is applied to exterior surfaces of the Saturn S-IV stage, IU, SMA, and electronic canister.

The requirements placed on the micrometeoroid detector panel thermal control coating were twofold. The radiometric properties had to be consistent with the thermal analysis requirements and the coating (thin compared to the capacitors) since a thick thermal control coating would interfere with the meteoroid statistical analysis. Candidate coatings were vapor-deposited silicon monoxide and Alodine. Cost estimates practically eliminated the former coating; coating of a minimum of 1200 target sheets would have been required for Pegasus A, B, and C. Since each sheet is about 0.5 square meters, it would be a major task to vacuum deposit the silicon monoxide. Alodine, selected by Fairchild-Hiller, required extensive development before a satisfactory coating was achieved. This Alodine coating, called MTL 200, satisfied all the imposed requirements.

## Laboratory Studies and Test

Detector panel laboratory studies. -Computer calculations have shown the detector panel orbital temperatures to be critical with respect to specifications for the case in which the panel is oriented broadside to the sun. A study was initiated to simulate this condition as nearly as possible with the present laboratory techniques.

A 0.1 $m^2$ detector panel was specially fabricated by Schjeldahl for this study. Eight thermocouples in two stacks of four each were embedded inside the panel during fabrication. The panel was situated in the thermal space chamber (Fig. 16), which is located in the Space Thermodynamics Branch of Research Projects Laboratory. The panel faced a quartz window through which it was illuminated by a carbon arc lamp. The lamp was switched on and off to simulate

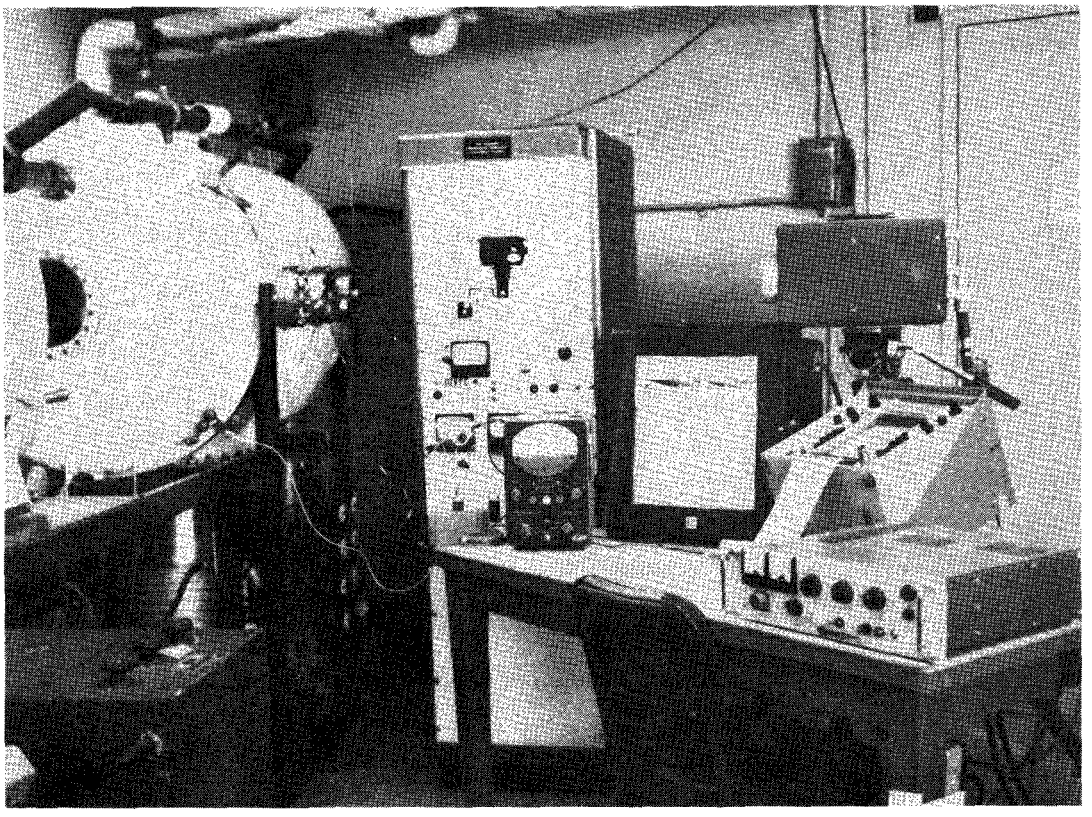

FIGURE 16. THERMAL SPACE CHAMBER

the shadow-sun condition of space. The intensity of the lamp was measured periodically with an Epply thermopile mounted on a rotary feedthrough. The intensity was found to vary about 10 percent in an unpredictable fashion. The chamber shroud was maintained at 77° K with $LN_2$, and the pressure fluctuated in the $10^{-6}$ to $10^{-7}$ torr range. Radiometric measurements were made on the Alodine surface at the thermocouple stacks before and after vacuum.

Figure 17 shows the measured temperatures for several runs. The maximum design limit of 398° K (250° F) was exceeded because the lamp intensity was greater than one sun. Calculations show remarkable agreement with theoretical results if the intensity spikes are smoothed. A computer program was written for a detailed study. Figure 18 shows the calculated temperature superimposed on the measured values. This study verified the thermodynamic model and the various thermophysical properties used in the thermal analysis of the detector panels.

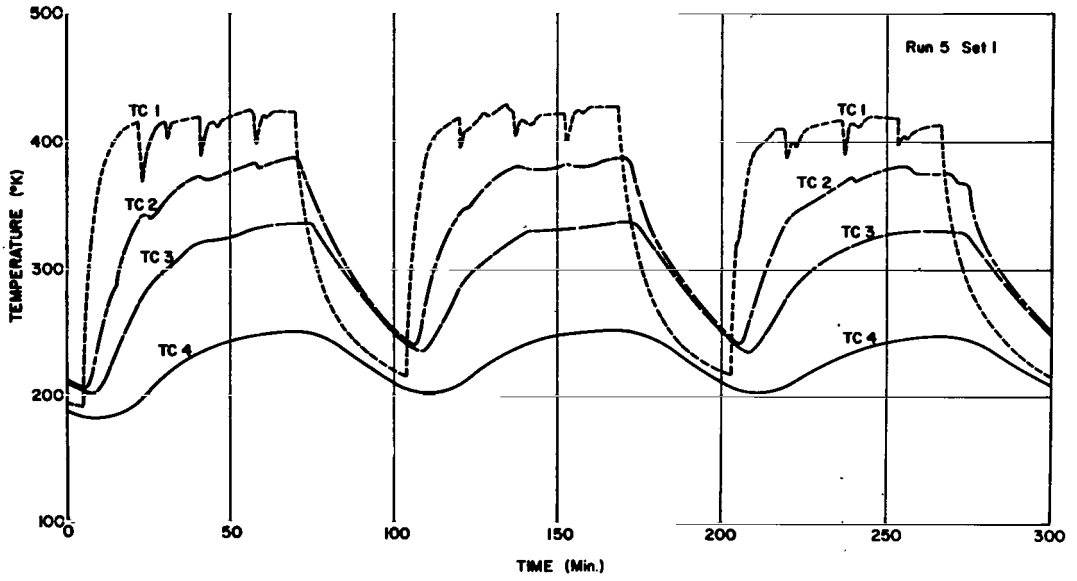


FIGURE 17. MEASURED DETECTOR PANEL TEMPERATURES

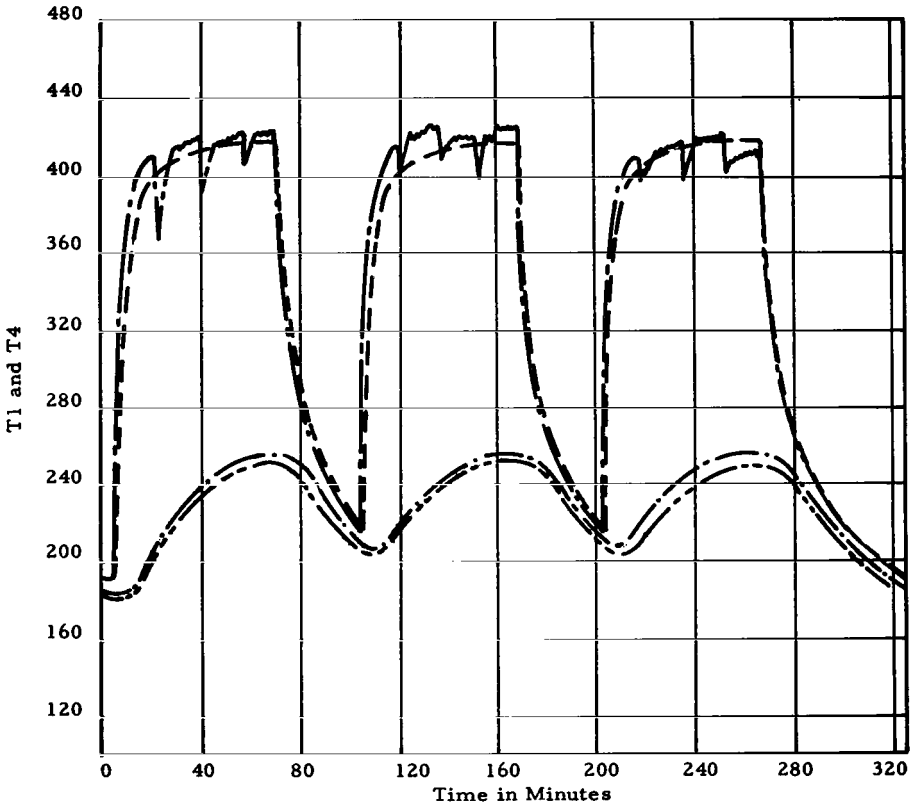


FIGURE 18. MEASURED AND CALCULATED DETECTOR PANEL TEMPERATURES

Electronic canister thermal vacuum orbital simulation. -A series of thermal vacuum orbital simulation tests was conducted at the Fairchild-Hiller facility. The principal test objective was to validate analytical predictions concerning component temperature levels as a function of orbital sink temperature. The test also served to verify the adequacy of the thermal blankets and textolite isolator clips in maintaining suitable temperature levels within various component dissipation ranges.

The test model consisted of the prototype electronic canister mounted in a prime center section modified slightly to fit the chamber. In general, all tubular structural members were retained to a distance of at least two feet outward from the canister superinsulation interface.

Orbital average sink temperatures corresponding to the computed incident fluxes were applied to external structure and canister surfaces through the use of 34 zoned electric heating blankets. These blankets completely enclosed the canister.

Approximately 201 thermocouples were used to instrument the test model. Thermocouples were located on each component and throughout the mounting plate and structure to allow a verification of the various heat paths.

The tests were conducted in two phases: (1) a cold case orbital simulation with minimum power dissipation corresponding to a 63-percent sunlight orbit, and (2) a hot case simulation corresponding to a 77-percent sunlight orbit with maximum component heat dissipation. During the transition between the cold and hot cases, all data were recorded. This made possible the verification of the computed thermal time constant.

The louver position was monitored by using a rotating sensing device. The device consisted of a shaft extension and disc combination which was affixed to the rotating blade. The disc had an elongated pie-shaped slot located eccentric to its axis of rotation. A light was passed through the slot and impinged upon a photoelectric cell. The output of the cell was then calibrated to read the louver position. The device was mounted on every third blade. This technique enabled the louver position to be correlated with the component and heat sink temperatures.

In performing the thermal vacuum test, extreme care was exercised to achieve realistic simulation of the orbital thermal environment. In any vacuum test there is a problem of eliminating the cold bias caused by the necessity of testing within a liquid nitrogen cooled shroud. Common practice in conducting a spacecraft system thermal vacuum test is to consider as negligible heat loss by conduction through service cables and wires. While this is usually a valid assumption for many spacecraft, it did not hold for Pegasus. Therefore, all instrumentation wires, test hardware, and electrical service wires were treated to

eliminate the unrealistic cold bias which they impose by virtue of their thermal interface with the electronics. In the Pegasus test, zoned heaters were provided for all test fixtures and service wires. Electrical wires and harness bundles were encased in separate heated conduits, which were monitored to achieve the space environment temperature. The end result was an accurate orbital simulation and test results that served to establish a high degree of confidence in analytical predictions. Both high and low temperature extremes were within 4° K of the analytical predictions based on the multinode mathematical model of the hardware.

Laboratory studies on Pegasus thermal control coatings. -Much effort was exerted in the laboratory evaluation of the space stability and optical properties of the Pegasus thermal control coatings. Studies were performed at MSFC, (both RPL and P&VE), Fairchild-Hiller, Schjeldahl, and Lockheed. Emphasis was placed on the Alodine and S-13 coatings because of their extreme importance to the success of the thermal design. Each was tested systematically to relate space degradation, manner of application, and prelaunch environmental effects. Table I shows the Alodine results.

The coatings were found to be extremely stable except that S-13 deteriorated after contamination. For this reason, the vehicle was washed just prior to countdown. Radiometric measurements were performed on the pad (Table II).

## TEMPERATURE MEASUREMENTS OF PEGASUS

The temperature measurements on the Pegasus spacecraft consist of two types. Nineteen temperature probes are of the pulse amplitude modulated variety, while six are pulse code modulated (digitized). The pulse amplitude modulated (PAM) temperatures are transmitted once each 15 seconds continuously. However, the PAM data are only obtained for periods of about 15 minutes since the spacecraft is in the field of view of a tracking station for only this short time. Initially, several stations tracked each Pegasus orbit for about two weeks. Thereafter, only one pass each orbit is tracked. The pulse code modulated data are stored onboard the satellite and are rapidly transmitted upon ground command (usually once per day).

Two of the digitized probes are located on the opposite faces of an uncharged meteoroid detector panel. The remaining digitized temperature measurement devices are located on special surfaces designed to study experimentally the radiometric properties of the Pegasus thermal control coatings. This device is called a space environmental effect sensor (SEES). There are nine temperature probes on the temperature-sensitive components inside the electronics canister,

TABLE I. LABORATORY RADIOMETRIC STUDIES ON ALODINE (MTL-3)

| THERMAL-VACUUM* | | | | | THERMAL-VACUUM* -ULTRAVIOLET** | | | | | | |
|---|---|---|---|---|---|---|---|---|---|---|---|
| Sample No. | $\epsilon_T$ Before | Temp °C | $\epsilon_T$ After | Sample No. | $\epsilon_T$ Before | $\alpha_s$ Before | Time ** ESH | Temp °C | $\epsilon_T$ After | $\alpha_s$ After | $\Delta\alpha_s/\epsilon_T$ |
| H | 0.57 | 110 | 0.51 | K | 0.68 | 0.463 | 300 | 85 | 0.64 | 0.471 | +0.055 |
| | 0.51 | 195 | 0.44 | L | 0.64 | 0.484 | 300 | 85 | 0.62 | 0.491 | +0.042 |
| I | 0.57 | 110 | 0.47 | M | 0.58 | 0.505 | 300 | 60 | 0.58 | 0.514 | +0.015 |
| J | 0.65 | 125 | 0.54 | N | 0.62 | 0.509 | 860 | 97 | 0.63 | 0.511 | -0.010 |
| | | | | O | 0.54 | 0.507 | 860 | 27 | 0.54 | 0.518 | +0.020 |
| | | | | P | 0.60 | 0.520 | 860 | 28 | 0.60 | 0.536 | +0.026 |
| | | | | Q | 0.67 | 0.451 | 1000 | 120 | 0.63 | 0.470 | +0.073 |
| | | | | R | 0.55 | 0.533 | 1000 | 137 | 0.52 | 0.543 | +0.075 |
| | | | | S | 0.51 | 0.531 | 1000 | 75 | 0.50 | 0.544 | +0.047 |

* $10^{-5}$ Torr

** ESH = equivalent sun hours of ultraviolet (0.2 - 0.4 microns)

TABLE II. SUMMARY OF SEVERAL ON-THE-PAD RADIOMETRIC SURVEYS ON PEGASUS-A

I. THE S-13 THERMAL CONTROL COATING (On the Service Module Adapter, Instrument Unit, and S-IV

A. Measurements of S-13 Coated Tabs placed near the Vehicle on-the-pad

1. $.22 \leq \alpha_s \leq .25$

2. $.82 \leq \epsilon_N \leq .88$

B. Measurements Made on the Service Module Adapter, Instrument Unit, and S-IV

1. $.16 \leq \alpha_s \leq .24$

2. $.81 \leq \epsilon_N \leq .86$

3. $.16 \leq \alpha_s \leq .19$ (measurements made just after vehicle was washed 7 days prior to launch)

II. THE ALODINE THERMAL CONTROL (On the Detector Panels)

A. Measurements Made on Alodine (MTL-3) Coated Tabs placed near Pegasus on-the-pad

1. $.51 \leq \alpha_s \leq .53$

2. $.53 \leq \epsilon_N \leq .58$

3. $\alpha_s/\epsilon_N \leq 1.0$

B. Measurements Made on the Detector Panels

1. $.50 \leq \alpha_s \leq .56$

2. $.53 \leq \epsilon_N \leq .65$

3. $\alpha/\epsilon \leq 1.0$

---

$\alpha_s$ Measurements were made with a Portable Gier Dunkle Reflectometer

$\epsilon_N$ Measurements were made with a Protable Lion Emittometer

two probes on the radiation detector package, a temperature probe on each of the four solar cell panels, three probes on the SMA skin, and a probe on the container of the thermal control coatings experiment.

The thermal data being received from these probes are being used to determine the temperature status for input into the evaluation of the spacecraft operation, to evaluate the effectiveness of the thermal design techniques employed to maintain proper temperature control of the temperature-sensitive components, to analyze the effect of the space environment on the thermal design, and to better determine, as far as possible, the thermal environment of space.

All of the temperature-sensitive components are well within their normal operating or design ranges on Pegasus A, B, and C (Table III).

TABLE III. RANGE OF PEGASUS TEMPERATURES

| COMPONENT | DESIGN RANGE (°K) | ACTUAL RANGE (°K) |
|---|---|---|
| Radiation Detector | 222° to 388° | 230° to 320° |
| Batteries | 272° to 322° | 290° to 314° |
| Other Electrical Component (in the Electronics Canister) | 262° to 332° | 275° to 330° |
| Solar Panels | 194° to 339° | 210° to 340° |
| Meteoroid Detector Panels | 167° to 394° | 225° to 385° |

The data are prepared graphically over both short and long periods. Within-orbit variations are studied with the short time graphs, and long trends are studied with the long time graphs. By superimposing the data from several consecutive orbits which are thermodynamically similar, the PAM temperature data are defined continuously for an orbit (Fig. 19). Notice the effect of the earth's shadow on the temperature response. Figure 20 shows an example of the data for several months.

Figures 21 and 22, respectively, show examples of the meteoroid detector panel temperatures while the spacecraft is spinning about the longitudinal axis and about the detector plane normal.

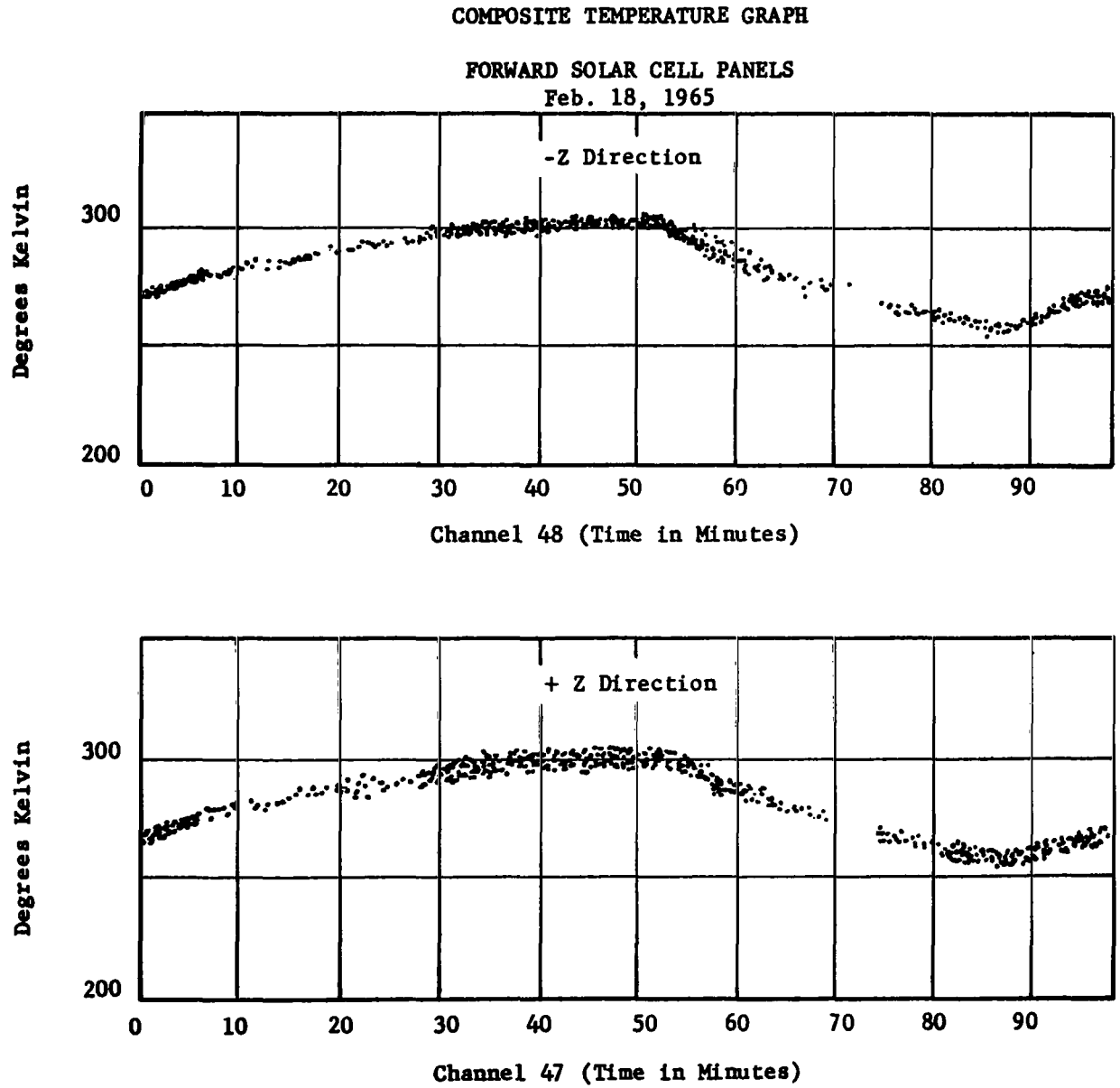


FIGURE 19. ORBITAL DATA: FORWARD SOLAR PANEL

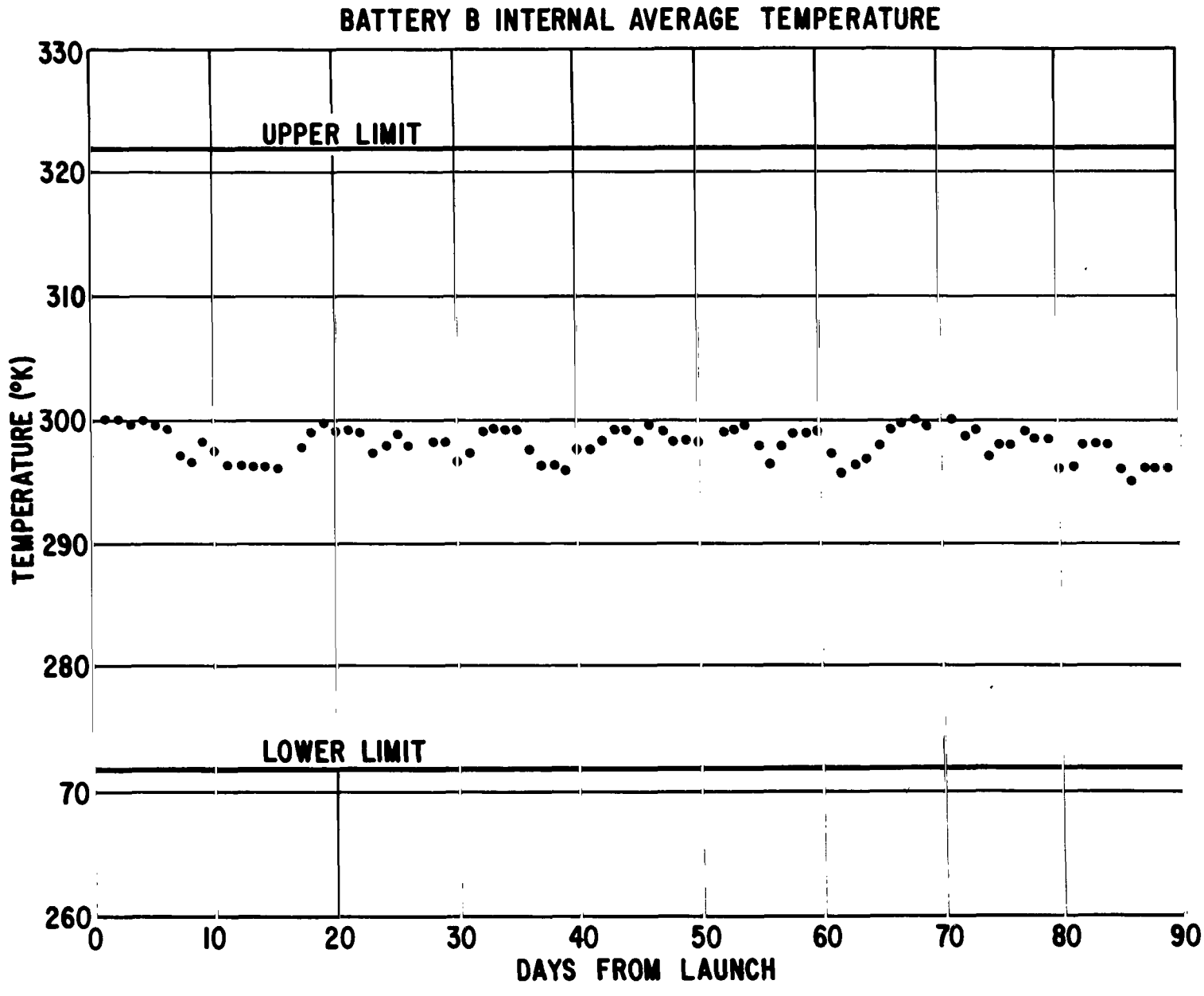


FIGURE 20. BATTERY ORBITAL TEMPERATURES

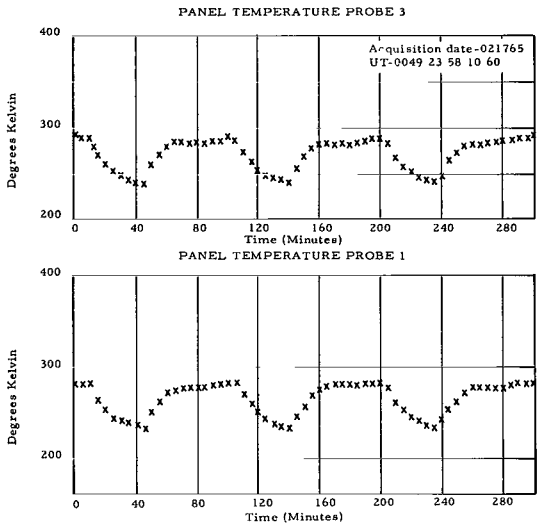


FIGURE 21. EARLY PANEL TEMPERATURE DATA

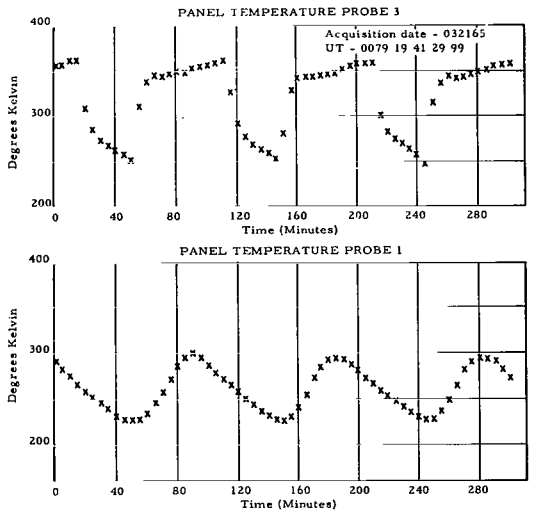


FIGURE 22. LATER PANEL TEMPERATURE DATA

The thermal design evaluation of the Pegasus involves studies of the degradation of the thermal control coatings such as those used on the SMA and the meteoroid detector panels, generation of calculated temperatures from heat balance analysis, comparison of predicted and actual temperatures, and evaluation of the active control louvers on the electronics canister.

Considerable interest has been aroused because of the unexpected doubling of the $\alpha_S/\epsilon_T$ ratio ($\alpha_S$ - solar absorptance, $\epsilon_T$ - infrared emittance) of the SMA, IU, and S-IV white paint (ZnO in Methyl Silicone). This could have a great effect on such projects as Apollo and LEM, which are more critically dependent upon stable $\alpha_S/\epsilon_T$ ratios. The SMA temperature probes show that the temperatures are much warmer than planned. To arrive at a satisfactory explanation of the unexpected temperatures, orbital data are being studied to define the $\alpha_S/\epsilon_T$ history of the SMA.

Preliminary analysis of the orbital data indicates that the louvers are functioning properly. Studies are in progress to define louver blade angles in orbit.

In addition to the meteoroid experiments carried aboard the spacecraft, there is a thermal surface experiment, using the SEES. The primary purpose of the SEES is to observe and measure the effects of the space environment on the radiometric characteristics of certain thermal control coatings. Each sensor package consists of four individual sensors (Fig. 23) consisting of a thin aluminum disc with a thermal control coating on the exterior surface. A resistance

thermometer is attached to the underside of the disc. Then a thin gold coat is deposited on the underside, lowering heat losses to the case. The disc is supported by thin Ti (6 Al 4 V) alloy rods, each 20 mil in diameter. This alloy has reasonable strength and low thermal conductivity.

Analysis of the Pegasus data is progressing. The $\alpha_s/\epsilon_T$ ratio of solar absorptance to infrared emittance is presented as a function of equivalent sun-time in Figure 24. The data were taken from Pegasus A orbits with the sensor

FIGURE 23. SPACE ENVIRONMENTAL EFFECT SENSORS

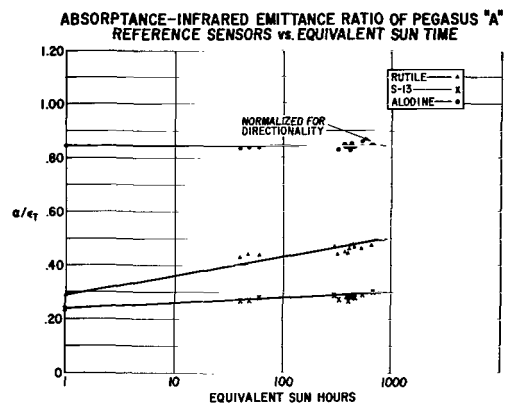


FIGURE 24. ORBITAL $\alpha_s/\epsilon_T$ MEASUREMENTS

normal (the sensor normal is parallel to the spacecraft spin-axis) facing the sun at points in the orbit where the earth is not visible to the sensors; thus, $\alpha_s/\epsilon_T$ is obtained from the steady-state disc temperature which is primarily a function of solar input. The irregular spinning of Pegasus B and C is hampering the thermal analysis of these spacecraft.

These data are given for the primary thermal control coatings with respect to the black reference coating. The Alodine coating has been very stable thus far. Since this coating has fairly strong directionality, the data are normalized for directionality.

Another interesting study being performed with the sensor data concerns the earth's albedo. Several orbits of data have been obtained where the plane of the sensor has remained 180° from the sun; thus, the dominant energy input is albedo in the sunlit portion of the orbit. Calculation of the albedo flux is being made with a spacial computer program.

Marshall Space Flight Center
National Aeronautics and Space Administration
Huntsville, Alabama, January 14, 1966

# APPENDIX

## Article I. The General Space Thermal Program*

This program includes subroutines for obtaining geometric and orbital parameters necessary to compute the many flux terms, and, simultaneously, solves a set of "n" calorimetric equations of the general form:

$$\dot{T}_i H_i = A_{1i}\alpha_i S + A_{2i}\alpha_i SB + A_{3i}\epsilon_i SE - A_{4i}\epsilon_i \sigma \left(\frac{T_i}{100}\right)^4 + \sum_{j=i}^{n} C_{ij}T_j + R_{ij}\left(\frac{T_i}{100}\right)^4 - T_i \sum_{j=i}^{n} C_{ij} - \left(\frac{T_i}{100}\right)^4 \sum_{j=i}^{n} R_{ij} + \dot{Q}_i$$

where

$T_i$ = temperature of node i

$\dot{T}_i = \frac{dT_i}{dt}$

$H_i$ = heat cap of node i

$C_{ij}$ = conductance between nodes i and j

$R_{ij}$ = radiance between nodes i and j

* The general computer program was developed by Research Projects Lab (-T) and Computation Laboratory (-P).

$\dot{Q}_i$ = internal heat of node i

$\alpha_i$ = solar absorptance of node i

$\epsilon_i$ = IR emittance of node i

S = insolation

B = maximum percent of S for albedo

E = maximum percent of S for earth's IR

$\sigma$ = Stefan-Boltzmann constant

$A_{1i}$ = area function for incident solar energy to node i

$A_{2i}$ = area function for incident albedo energy to node i

$A_{3i}$ = area function for incident earth is IR to node i

$A_{4i}$ = radiating area of node i.

## Article II. Computer Program Describing the MMC* Detector Panels

The functions incorporated into the General Space Thermal Program for study of the detector panels follow:

Area Functions

a. Solar

$A_{11} = A_{41} D \cos (MAS)$

$A_{11} = 0$ if MAS > 90°

$A_{12} = 0$

$A_{13} = 0$

* Micrometeroid Measurement Capsule (Ref. p. 3).

$A_{14} = A_{44}\, D \cos\,(180\text{-MAS})$

$A_{14} = 0$ if supp MAS > 90°

b. Albedo

$A_{21} = A_{41}\ (F\gamma_{1_r})\ \cos\ (RAS)$

$A_{21} = 0$ if RAS > 90°
$\gamma_1 = 180°$ -RAM

$A_{22} = 0$

$A_{23} = 0$

$A_{24} = A_{44}(F\gamma_{4_r})\ \cos\ (RAS)$

$A_{24} = 0$ if RAS > 90°
$\gamma_4 = RAM$

c. Earth's IR

$A_{31} = A_{41}\ F_{\gamma_{1_r}}$

$A_{32} = 0$

$A_{33} = 0$

$A_{34} = A_{44}\ F_{\gamma_{1_r}}$

d. Stefan-Boltzmann radiation

$A_{41} = 1$

$A_{42} = 0$

$A_{43} = 0$

$A_{44} = 1$

e. Generated heat fluxes

all $\dot{Q}_1 = 0$

f. Conductance

$C_{12} = C_{21} = 4.6$ cal/hr°K

$C_{23} = C_{32} = 2.3$

$C_{34} = C_{43} = 1.4$

g. Heat capacities

$H_1 = H_4 = .36$

$H_2 = H_3 = .22$

h. Orbital parameters (predicted)

Rp = 6778 km

i = 31.8°

e = .0076

Tx = 63 to 78

$\Omega = 0$

$\omega = 90$

Ps = 90 .

# REFERENCES

1. Plamondon, J. A.: Analysis of Movable Louvers for Temperature Control. J. Spacecraft and Rockets, vol. 3, no. 5, Sept.-Oct. 1964, p. 492.



NASA-Langley, 1966 M414

*"The aeronautical and space activities of the United States shall be conducted so as to contribute . . . to the expansion of human knowledge of phenomena in the atmosphere and space. The Administration shall provide for the widest practicable and appropriate dissemination of information concerning its activities and the results thereof."*

—NATIONAL AERONAUTICS AND SPACE ACT OF 1958

# NASA SCIENTIFIC AND TECHNICAL PUBLICATIONS

TECHNICAL REPORTS: Scientific and technical information considered important, complete, and a lasting contribution to existing knowledge.

TECHNICAL NOTES: Information less broad in scope but nevertheless of importance as a contribution to existing knowledge.

TECHNICAL MEMORANDUMS: Information receiving limited distribution because of preliminary data, security classification, or other reasons.

CONTRACTOR REPORTS: Technical information generated in connection with a NASA contract or grant and released under NASA auspices.

TECHNICAL TRANSLATIONS: Information published in a foreign language considered to merit NASA distribution in English.

TECHNICAL REPRINTS: Information derived from NASA activities and initially published in the form of journal articles.

SPECIAL PUBLICATIONS: Information derived from or of value to NASA activities but not necessarily reporting the results of individual NASA-programmed scientific efforts. Publications include conference proceedings, monographs, data compilations, handbooks, sourcebooks, and special bibliographies.

***Details on the availability of these publications may be obtained from:***

**SCIENTIFIC AND TECHNICAL INFORMATION DIVISION**

**NATIONAL AERONAUTICS AND SPACE ADMINISTRATION**

**Washington, D.C. 20546**